

Stress Analysis of Bilayer Composite Materials with Various Poisson Ratio

Yeasin Bhuiyan¹, Md. Abdus Salam Akanda³, Karim Egab², Hassan Raheem Hassan² and Saad K. Oudah¹

¹University of South Carolina, Columbia, SC-29208, USA

²University of Mazaya, Nasiriyah-5060, Iraq

³Bangladesh University of Engineering and Technology, Dhaka, Bangladesh

*Corresponding Author Email: engkarim.mech@gmail.com

Abstract

Composites materials are needed because of the widely used in structures and designs. In this work, the stress analysis of two-dimensional bilayer composite materials has a different Poisson ratio have studied. The materials under consideration are assumed to be perfectly bonded together. Finite difference method is used for the solution of two-dimensional elastic problems. In each layer of the composite, the mechanical properties are isotropic. The results are observed that the results agree well within the acceptable limit, which also confirms the reliability of the finite difference method. Changing in Poisson's ratio in any layer has significant effects on the results of all layers of the bilayer composite. Due to the mathematical expressions of stresses and displacements for two-dimensional elastic problems, the study of the effects of Poisson's ratio has a significant influence.

Keywords: stress analysis, composite material, Poisson ratio and FEM.

1. Introduction

The composite material can be formed by combining materials to form an overall structure that has better than the individual components. Various methods have been used to define the bilayer materials to obtain a better mechanical property [1-3]. Graphene has a better mechanical properties compared to other materials. The Graphene has a breaking strength over 100 times greater than a hypothetical steel film for the same thickness [4, 5]. The graphene bilayer was two layers of graphene having different properties. In addition, the graphene has interesting mechanical and electrical properties [7,6]. The resulted graphene layers make the material promising candidates for optoelectronic and nanoelectronic applications. Stress analysis could be performed on the bilayer graphene under mechanical loading. Numerous cases [8] in which the elementary methods of strength of materials are inadequate to provide satisfactory and accurate information regarding stress distribution in engineering structures.

Long et al. [9] predicted the nominal stress-strain curves of a multi-layered composite material by FEM Analysis. The analytic solution performed stress-strain analysis of the laminates with orthotropic layers using Classical Laminate theory considering the thermal loading [10]. Some researchers have used finite element technique for stress analysis of some layered materials [11]. Challenges with various mechanical loadings were not discussed in these studies. The determination of the stresses for composite lamina considering directional mechanical properties was performed [12]. Therefore, stress analysis in layer to layer materials as well as at the interfaces is yet to be solved by this approach.

In this work, development of finite difference scheme for the elastic body and boundary conditions at the interface of the bilayer composite isotropic materials. The investigation of displacement and stress distribution in the layers as well as at the interface were

discussed. Also, the stresses in composite materials for different combinations were analyzed.

2. Mathematical Model and Procedure

In the analysis, the bilayer composite materials undergoing the action of mechanical loadings are perfectly elastic and the deformations are very small. The displacements, strains, and stresses in a deformable body are related to each other. In this analysis, the deformations of the elastic body are considered very small. Hence, the deformation is elastic. The state of strain at any point could be completely defined by six components of strain: ϵ_x , ϵ_y , ϵ_z , γ_{xy} , γ_{yz} , and γ_{zx} . By definition the normal and shear strain can be given by [12]:

$$\epsilon_x = \frac{\partial u_x}{\partial x}, \epsilon_y = \frac{\partial u_y}{\partial y}, \epsilon_z = \frac{\partial u_z}{\partial z} \quad (1)$$

$$\gamma_{xy} = \frac{\partial u_x}{\partial y} + \frac{\partial u_y}{\partial x}, \gamma_{yz} = \frac{\partial u_y}{\partial z} + \frac{\partial u_z}{\partial y}, \gamma_{zx} = \frac{\partial u_x}{\partial z} + \frac{\partial u_z}{\partial x} \quad (2)$$

The generalized Hooke's law suggests that each of the stress components is the linear function of the strain components.

$$\epsilon_x = \frac{1}{E} [\sigma_x - \mu(\sigma_y + \sigma_z)], \epsilon_y = \frac{1}{E} [\sigma_y - \mu(\sigma_x + \sigma_z)]$$

$$\epsilon_z = \frac{1}{E} [\sigma_z - \mu(\sigma_x + \sigma_y)] \quad (3)$$

Where E is the modulus of elasticity and μ is the Poisson's ratio. The following equations can be obtained [12] for static equilibrium

$$\begin{aligned} \frac{\partial \sigma_{xx}}{\partial x} + \frac{\partial \sigma_{xy}}{\partial y} + \frac{\partial \sigma_{xz}}{\partial z} + X &= 0 \\ \frac{\partial \sigma_{yy}}{\partial y} + \frac{\partial \sigma_{xy}}{\partial x} + \frac{\partial \sigma_{yz}}{\partial z} + Y &= 0 \\ \frac{\partial \sigma_{zz}}{\partial z} + \frac{\partial \sigma_{xz}}{\partial x} + \frac{\partial \sigma_{yz}}{\partial y} + Z &= 0 \end{aligned} \quad (4)$$

For plane stress condition the cubic element reduces to a thin rectangular block and nobody forces acting on that block. Hence the equilibrium equations yield to

$$\begin{aligned} \frac{\partial \sigma_{xx}}{\partial x} + \frac{\partial \sigma_{xy}}{\partial y} &= 0 \\ \frac{\partial \sigma_{yy}}{\partial y} + \frac{\partial \sigma_{xy}}{\partial x} &= 0 \end{aligned} \quad (5)$$

At the boundary they must be in equilibrium with external forces on the boundary and the external forces is considered as the continuation of the internal stress distribution. So the conditions of equilibrium at the boundary can be written as [12]:

$$\begin{aligned} \sigma_n &= \sigma_{xx} \cdot l^2 + \sigma_{yy} \cdot m^2 + 2\sigma_{xy} \cdot l m \\ \sigma_t &= \sigma_{xy} \cdot (l^2 - m^2) + (\sigma_{yy} - \sigma_{xx}) \cdot l m \end{aligned} \quad (6)$$

Where σ_n and σ_t are the normal and tangential components of the surface forces acting on the boundary per unit area and l, m are the direction cosines of the normal to the surface. The normal component of displacement u_n and the tangential component u_t acting on the boundary surface can be expressed by

$$\begin{aligned} u_n &= u_x \cdot l + u_y \cdot m \\ u_t &= u_y \cdot l - u_x \cdot m \end{aligned} \quad (7)$$

To determine the stress in the two-dimensional elastic body, it is necessary to find the solution of the equilibrium equations (Eq. 5). For two time two-dimensional tree strain components can be expressed in terms of regarding of displacement components as

$$\varepsilon_x = \frac{\partial u_x}{\partial x}; \quad \varepsilon_y = \frac{\partial u_y}{\partial y}; \quad \gamma_{xy} = \frac{\partial u_x}{\partial y} + \frac{\partial u_y}{\partial x} \quad (8)$$

Since these three strain components are expressed by two functions only, they cannot be related arbitrarily among themselves. There exists a certain relationship among the strain components, which is expressed as,

$$\frac{\partial^2 \varepsilon_x}{\partial y^2} + \frac{\partial^2 \varepsilon_y}{\partial x^2} = \frac{\partial^2 \gamma_{xy}}{\partial x \partial y} \quad (9)$$

This differential relation is called the condition of compatibility. It must be satisfied by the strain components to ensure the existence of functions u_x and u_y connected with the strain components by Eq. 8. Elimination of strains regarding stresses, equation nine yields to

$$\left(\frac{\partial^2}{\partial x^2} + \frac{\partial^2}{\partial y^2} \right) (\sigma_x + \sigma_y) = 0 \quad (10)$$

The method of solving these equations is through the introduction of a function $\phi(x,y)$, known as Airy stress function, defined as

$$\sigma_x = \frac{\partial^2 \phi}{\partial y^2}, \quad \sigma_y = \frac{\partial^2 \phi}{\partial x^2}, \quad \sigma_{xy} = \frac{\partial^2 \phi}{\partial x \partial y} \quad (11)$$

which satisfies equations (Eq. 6) and transforms the equation (Eq. 10) into

$$\frac{\partial^4 \phi}{\partial x^4} + 2 \frac{\partial^4 \phi}{\partial x^2 \partial y^2} + \frac{\partial^4 \phi}{\partial y^4} = 0 \quad (12)$$

Mathematical Formulation regarding Displacement Potential Function

The equilibrium equations for two-dimensional elastic problems regarding displacements components are as follows

$$\begin{aligned} \frac{\partial^2 u}{\partial x^2} + \left(\frac{1-\mu}{2} \right) \frac{\partial^2 u}{\partial y^2} + \left(\frac{1+\mu}{2} \right) \frac{\partial^2 v}{\partial x \partial y} &= 0 \\ \frac{\partial^2 v}{\partial y^2} + \left(\frac{1-\mu}{2} \right) \frac{\partial^2 v}{\partial x^2} + \left(\frac{1+\mu}{2} \right) \frac{\partial^2 u}{\partial x \partial y} &= 0 \end{aligned} \quad (13)$$

A new potential function approach involves an investigation of the existence of a function defined regarding the displacement components. In this approach, an attempt had been made to reduce the problem to the determination of a single variable. A function $\psi(x,y)$ is thus defined regarding displacement components as, [12]

$$u = \frac{\partial^2 \psi}{\partial x \partial y}, \quad v = - \left[\left(\frac{1-\mu}{1+\mu} \right) \frac{\partial^2 \psi}{\partial y^2} + \left(\frac{2}{1+\mu} \right) \frac{\partial^2 \psi}{\partial x^2} \right] \quad (14)$$

with this definition of $\psi(x,y)$, the first of the two equations (13) is automatically satisfied. Therefore, ψ has only to satisfy the second equation. Thus, the condition that ψ has to satisfy is

$$\frac{\partial^4 \psi}{\partial x^4} + 2 \frac{\partial^4 \psi}{\partial x^2 \partial y^2} + \frac{\partial^4 \psi}{\partial y^4} = 0 \quad (15)$$

Therefore, the problem is reduced to the evaluation of a single variable $\psi(x,y)$ from the above bi-harmonic partial differential equation.

In order to solve the problem by solving for the function ψ of the bi-harmonic equation (Eq. 15), the boundary conditions should be expressed regarding ψ . The boundary conditions are known restraints and loadings, that is, known values of components of stresses and displacements at the boundary. The relation between known functions and the potential function ψ at the boundary are [12]

$$\begin{aligned} u &= \frac{\partial^2 \psi}{\partial x \partial y}, \quad v = - \left[\left(\frac{1-\mu}{1+\mu} \right) \frac{\partial^2 \psi}{\partial y^2} + \left(\frac{2}{1+\mu} \right) \frac{\partial^2 \psi}{\partial x^2} \right] \quad (16) \\ \sigma_x &= \frac{E}{(1+\mu)^2} \left[\frac{\partial^3 \psi}{\partial x^2 \partial y} - \mu \frac{\partial^3 \psi}{\partial y^3} \right], \quad \sigma_y = - \frac{E}{(1+\mu)^2} \left[\frac{\partial^3 \psi}{\partial y^3} + (2 + \mu) \frac{\partial^3 \psi}{\partial x^2 \partial y} \right] \quad (17) \\ \sigma_{xy} &= \frac{E}{(1+\mu)^2} \left[\mu \frac{\partial^3 \psi}{\partial x^2 \partial y} - \frac{\partial^3 \psi}{\partial x^3} \right] \end{aligned}$$

From the above expressions, the boundary conditions are concerned, either known restraints, stresses and combinations of stresses and displacements. The boundary conditions converted to finite difference expressions regarding ψ at the boundary. Considering pragmatic applicability, the rectangular components are converted into normal and tangential components, as these are known at the boundary using the following relationship (Eq. 7 and Eq. 9) [12].

2.1 Validation

The validation of program consists of a bilayer composite material under axial loading as shown in FIGURE 1. The program solves the displacement and stress distributions. The problem is considered as plane stress problem. The left side of the bilayer composite material is fixed while the right side is under uniform normalized tensile stress. The geometry of the problem is square having $a/b=1.0$ and $a=b=25$ unit. This solution for stress and displacement distribution by using finite difference method and the finite element method is obtained by taking $\mu_1=0.32$, $\mu_2=0.28$.

The mesh size selected for FDM analysis is 0.02 as shown in FIGURE 4.2 i.e, mesh length, $h=0.5$. In the mesh sensitivity curve for FEM analysis, as shown in FIGURE 4.3.

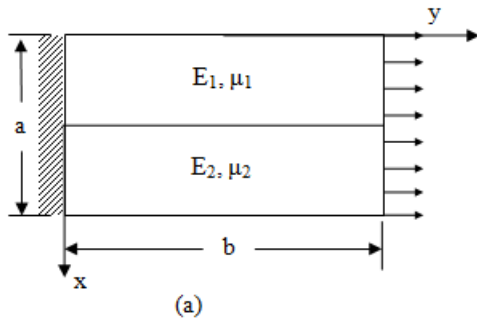


Fig. 1: Bilayer material under axial loading

In both FEM and FDM analysis, u and v are continuous over the bilayer composite. However, there are two values of each stress component one is for upper material and one is for lower material. Although there is a single nodal point at the interface it is a perfectly bonded two nodal point, two nodal points from top and lower by both the method. The two values of each stress component are obtained and the discontinuity in the distribution of stress at the connection point of the composite material is obtained.

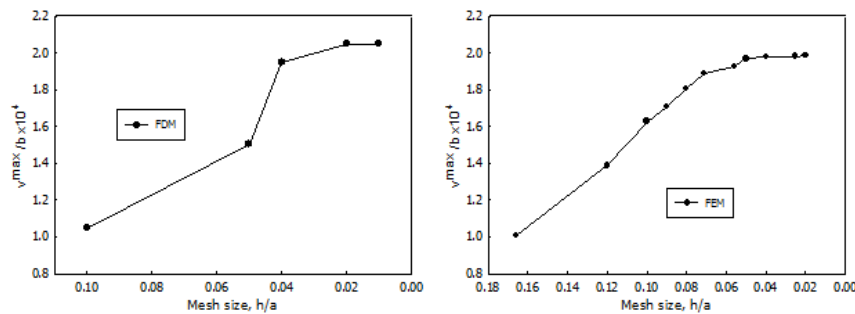


Fig. 2: (a) Variation of maximum displacement (v_{max}/b) with mesh size by FDM (b) Variation of maximum displacement (v_{max}/b) with mesh size by FEM.

The distribution of σ_{xy} as shown in FIGURE 4.6 matches up with each other by FDM and FEM method in different sections of the bilayer except at the top and bottom boundary points of section at $y/b=0.0$. The upper corner point could be considered at the both top and left boundary. Similarly, the lower corner point could be considered at the both bottom and left boundary. If top boundary condition is applied at the upper corner point, there is mismatch in results of boundary point by FDM and FEM. In FDM, there is provision to apply either of the two boundary conditions at the corner points. If left boundary conditions are applied at the upper and lower corner points, the FDM result becomes consistent with the FEM results. The distribution of σ_y at various sections of

The bilayer composite by FDM method is shown in FIGURE 4.8. It indicates that for this particular problem stress at section $y/b=0.0$ is very significant as compared to the other sections of the material. At other sections of the bilayer composite, the variation of the stress σ_y is very small and could not be discerned. Figure 4. shows that at $y/b= 0.0, 1.0$ and 2.4 . At $y/b=0.0$, the distribution of stress σ_y by FDM and FEM methods matches up with each other except at the upper and lower boundary points and at interface points as shown in FIGURE 4.10. The FEM result shows smaller value of stress σ_y at the boundary corner points (most critical point in engineering point of view as it correspond the highest stress) than FDM result. FDM result for distribution of σ_y exactly matches up with FEM result.

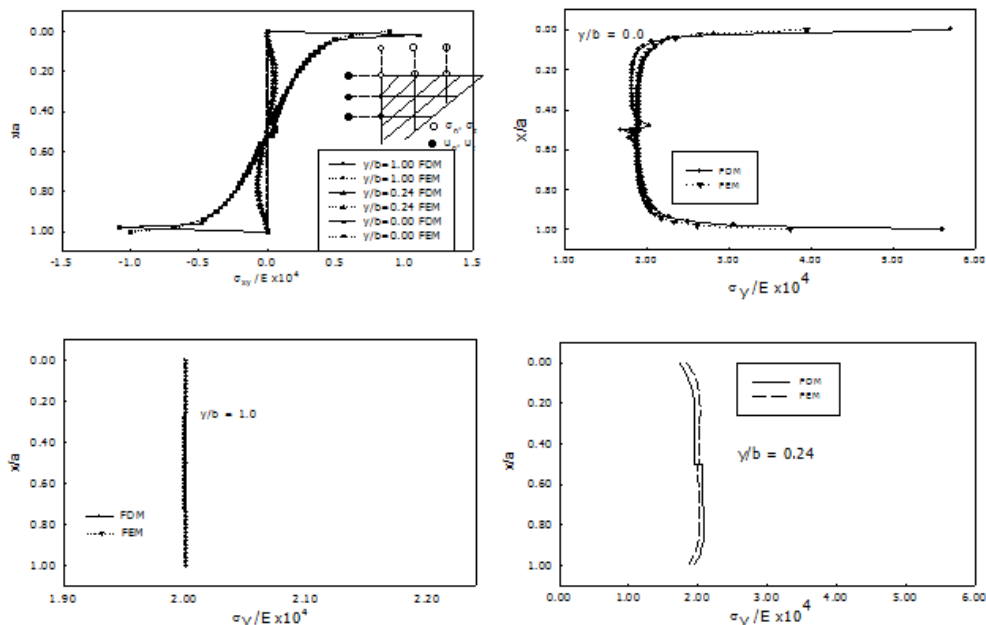


Fig. 3: (a) Comparison of normalized shear stress distribution at different sections of the bilayer composite (b) Comparison of normal stress (σ_y) distribution at $y/b=0.0$. (c) Comparison of normal stress (σ_y/E) distribution at $y/b=1.0$. (d) Comparison of normal stress (σ_y) distribution at $y/b=0.24$.

3. Result and Discussion

The distribution of stress and displacement is obtained for various combinations of material properties as well as for various types of boundary conditions. The stress and displacement distributions at the interface are also analyzed. The effect of Poisson's ratio on the stress and displacement distribution is studied. Several combinations of material are taken into consideration. Keeping the constant Poisson's ratio in the upper material, Poisson's ratio has been changed in the lower material. For pragmatic purpose, the changes are limited to $\mu_2 = 0.2$ to 0.4 for lower material and for upper material $\mu_1 = 0.3$. At a particular section $y/b=0.24$, the normalized displacement component (u/a) distribution for different Poisson's ratios of the bilayer composite is shown in FIGURE 4.

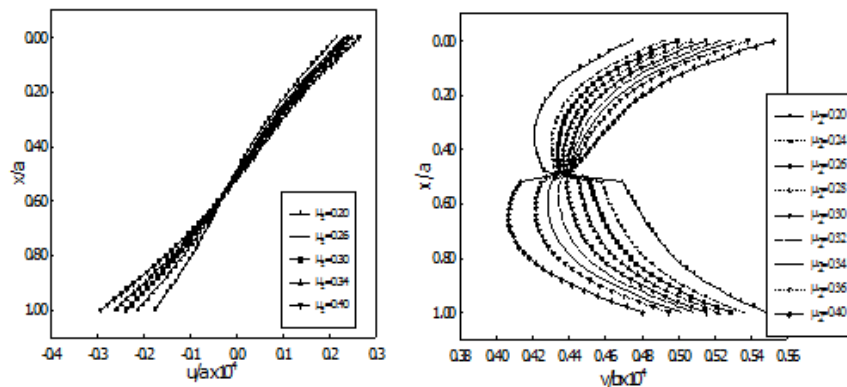


Fig. 4: (a) Variation of displacement component (u/a) for different Poisson's ratios at $y/b=0.24$ of the bilayer composite. (b) Variation of displacement component (v/b) for different Poisson's ratios at $y/b=0.24$ of the bilayer composite.

FIGURE 5 depicts the variation of normalized normal stress (σ_x/σ_{y0}) for different Poisson's ratios at $y/b=0.24$ of the bilayer composite. It shows that there is trivial change in normal stress (σ_x) distribution in the upper material where Poisson's ratio is constant. However, in the lower material, the normal stress (σ_x) increases as Poisson's ratio increases. For all cases of different Poisson's ratios in upper and lower material, there is bumping at the interface. It is noted that normal stress (σ_x) decreases more as Poisson's ratio decreases from 0.3 to 0.2 than it increases when Poisson's ratio increases from 0.3 to 0.4 . The variation of normalized normal stress (σ_y/σ_{y0}) for different Poisson's ratios at $y/b=0.24$ of the bilayer.

Composite is shown in FIGURE 5. It shows that for same Poisson's ratio in the upper and lower material the normal stress (σ_y) distribution is exactly symmetrical about the interface line. When Poisson's ratio in the lower material decreases the normal stress (σ_y) decreases in the lower material but increases in the upper material and the opposite phenomenon occurs when Poisson's ratio increases. For the same amount of increment and decrement of Poisson's ratio from 0.3 causes higher bumping at the interface during the decrement than the increment. It could be noted that the wavy nature in the curve of normal stress (σ_y) distribution is more where the Poisson's ratio is less as compared to each other.

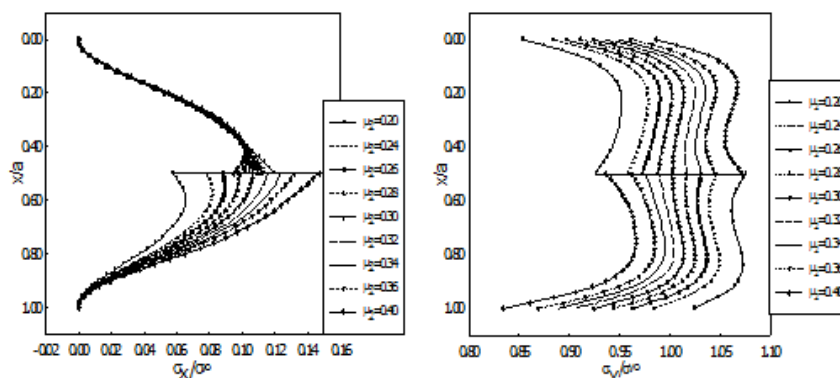


Fig. 5: (a) Variation of normal stress (σ_x/σ_{y0}) for different Poisson's ratios at $y/b=0.24$ of the bilayer composite (b) Variation of normal stress (σ_y/σ_{y0}) for different Poisson's ratios at $y/b=0.24$ of the bilayer composite.

FIGURE 6 illustrates the variation of normalized shear stress (σ_{xy}/σ_{y0}) for different Poisson's ratios at $y/b=0.24$ of the bilayer composite. In this FIGURE less number of Poisson's ratios is taken for comparison to avoid the clumsiness of the FIGURE as the variation of shear stress (σ_{xy}) is minimal. It shows that when Poisson's ratio is lower in the lower material. The magnitude of

shear stress (σ_{xy}) is lower in both materials and in case of higher Poisson's ratio in the lower material the magnitude of shear stress (σ_{xy}) is lower. It is noted that the shear stress (σ_{xy}) distribution is anti-symmetric and at the top and bottom boundary the shear stress satisfies the boundary condition.

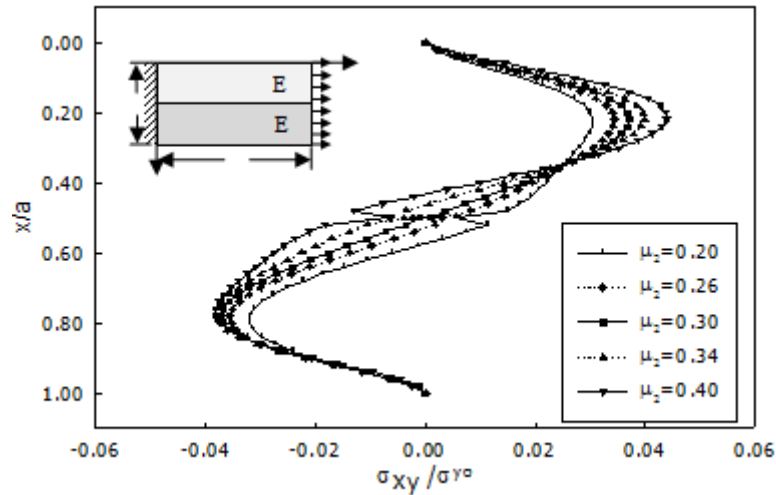


Fig. 6: Variation of shear stress (σ_{xy}/σ_{y0}) for different Poisson's ratios at $y/b=0.24$ of the bilayer composite.

The variation of normalized displacement component (u/a) for different Poisson's ratios at $y/b=0.50$ of the bilayer composite is shown in FIGURE 7. It shows that, the intersecting point of the displacement component (u/a) distribution curve shifts to the right as compared to that in section $y/b=0.24$. The distinction of the variation of displacement component (u/a) is more prominent in

the upper material as compared to that in section $y/b=0.24$. FIGURE 7 represents the variation of normalized displacement component (v/b) for different Poisson's ratios at $y/b=0.50$ of the bilayer composite. It shows that displacement component (v/b) is higher in the material of lower Poisson's ratio.

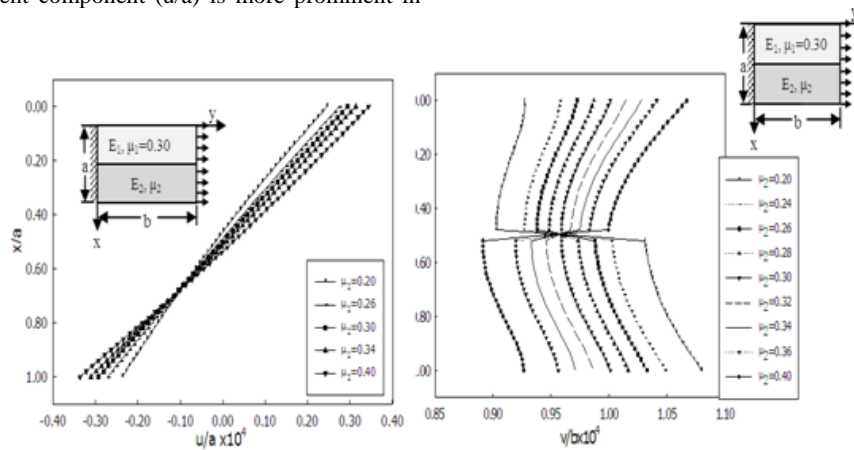


Fig.7: (a) Variation of displacement component (u/a) for different Poisson's ratios at $y/b=0.50$ of the bilayer composite (b) Variation of displacement component (v/b) for different Poisson's ratios at $y/b=0.50$ of the bilayer composite.

Variation of normalized normal stress (σ_y/σ_{y0}) for different Poisson's ratios at $y/b=0.50$ of the bilayer composite is represented in FIGURE 8. The wavy nature of the normal stress (σ_y) distribution is less as compared to that in section $y/b=0.24$ as depicted in FIGURE 5. FIGURE 8 represents the variation of normalized normal stress (σ_x/σ_{y0}) for different Poisson's ratios at $y/b=0.50$ of the bilayer composite. As shown in this FIGURE, the normal stress (σ_x) distribution is discerned in the upper material

that could not be discerned in case of section $y/b=0.24$. There is bumping in the normal stress (σ_x) for all cases of different Poisson's ratios in the upper and lower material. For the same Poisson's ratio in the upper and lower material, the normal stress (σ_x) distribution is symmetrical about the interface line.

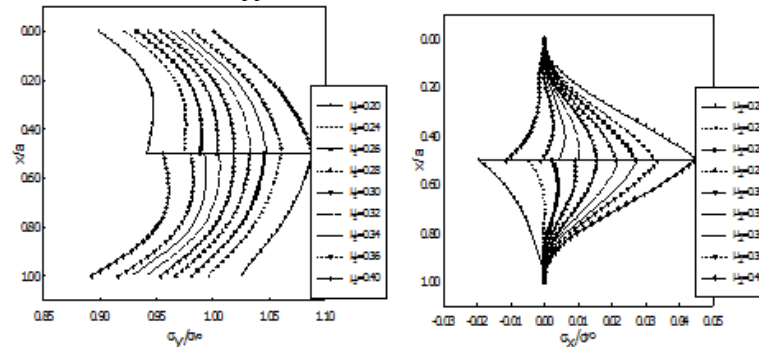


Fig. 8: (a) Variation of normal stress (σ_y/σ_{y0}) for different Poisson's ratios at $y/b=0.50$ of the bilayer composite (b) Variation of normal stress (σ_x/σ_{y0}) for different Poisson's ratios at $y/b=0.50$ of the bilayer composite.

The normalized shear stress (σ_{xy}/σ_{y0}) distribution for different Poisson's ratios at $y/b=0.50$ of the bilayer composite is represented in FIGURE 9. Unlike at section $y/b=0.24$, the shear

stress (σ_{xy}) is negative in both upper and lower material for Poisson's ratio $\mu_2 = 0.20$ and 0.26 . It shows that the magnitude of shear stress (σ_{xy}) is higher where the Poisson's ratio is higher.

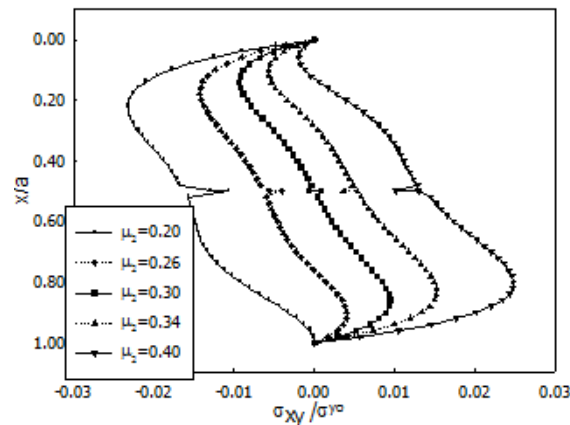


Fig. 9: Variation of shear stress (σ_{xy}/σ_{y0}) for different Poisson's ratios at $y/b=0.50$ of the bilayer composite.

4. Conclusion

The stress and displacement distributions are presented in the present analysis for various combinations of mechanical properties and loadings. The stresses have a pumping effect at the interface due to different mechanical properties. The variation of Poisson's ratio in the lower material has a significant effect on the distributions of stresses and displacements. The material with lesser Poisson's ratio experiences higher normalized normal stress in the direction of the tensile load than the material with greater Poisson's ratio. However, in case of normalized normal stress in the perpendicular direction of tensile loading at the interface, the material with lesser Poisson's ratio experiences less normalized normal stress.

References

- [1] Zabulionis D., "Stress and strain analysis of a bilayer composite beam with interlayer slip under hygrothermal loads", Scientific Journal "MECHANIKA", Nr.6(56), ISSN 1392 – 1207, pp 5-12, 2005.
- [2] Wallis G. and Pomerantz, D. I., "Field Assisted Glass-Metal Sealing". Journal of Applied Physics 40 (10). pp. 3946–3949, 1969.
- [3] P. Nitzsche and K. Klange and B. Schmidt and s. Grigull and U. Kreissig and B. Thoms and K. Herzog (1998). "Ion Drift Processes in Pyrex Type Alkali-Borosilicate Glass during Anodic Bonding". Electrochemical Society 145 (5). pp. 1755–1762.
- [4] http://www.nobelprize.org/nobel_prizes/physics/laureates/2010/advanced-physics-prize2010.pdf
- [5] Lee, C. et al. (2008). "Measurement of the Elastic Properties and Intrinsic Strength of Monolayer Graphene". Science 321 (5887): 385–8.
- [6] Min, Hongki; Sahu, Bhagawan; Banerjee, Sanjay; MacDonald, A. (2007). "Ab initio theory of gate induced gaps in graphene bilayers". Physical Review B 75 (15).
- [7] Barlas, Yafis; Côté, R.; Lambert, J.; MacDonald, A. H. (2010). "Anomalous Exciton Condensation in Graphene Bilayers". Physical Review Letters 104 (9)
- [8] Ahmed, S. R., "Numerical solution of mixed boundary value elastic problems", M. Sc. Thesis, Bangladesh University of Engineering and Technology, Bangladesh, 1993.
- [9] Long L., Iwasaki S., Yin F. and Nagai K. "Prediction of Nominal Stress-Strain Curves of a Multi-Layered Composite Material by FE Analysis", Materials Transactions, Vol. 51, No. 12, pp. 2188-2195, 2010
- [10] Sevecek O., Pletz M., Bermejo R., Supancic P. "Analytical Stress-Strain analysis of the laminates with orthotropic (isotropic) layers using Classical Laminate Theory", Materials Center Leoben Forschung GmbH, Presentation, 2011.
- [11] Wang Z., Wang W., Wang H. and Hu Y., "Stress Analysis on Layered Materials in Point Elastohydrodynamic-Lubricated Contacts", Tribology Letters (Springer), Vol. 35, Issue 3, pp. 229-244, 2009.
- [12] Alam, M. T., Akanda, M.A.S and Mandal, A.C., "Stress analysis of composite lamina having a square hole by finite difference technique", Proceedings of International Conference on Mechanical & Manufacturing Engineering, pp. 1-6, Johor Bahru, Malaysia, May 21-23, 2008.